Control of Kirchhoff vortices by a resonant strain

L. Friedland*
Racah Institute of Physics, Hebrew University of Jerusalem, 91904 Jerusalem, Israel
(Received 17 September 1998; revised manuscript received 28 December 1998)

It is shown that placing a Kirchhoff vortex in a weak resonant strain having uniform, but oscillating strain rate with chirped oscillation frequency, allows adiabatic control of the axis ratio $\rho=a/b$ and rotation phase of the vortex. The phenomenon has a threshold on the amplitude of oscillations of the strain rate and is due to the persisting nonlinear phase locking (autoresonance) between the elliptic vortex and the adiabatically varying straining flow. [S1063-651X(99)06104-8]

PACS number(s): 47.32.Cc

I. INTRODUCTION

Kirchhoff vortex [1] is a famous two-dimensional vortex patch solution in ideal fluids. It has constant vorticity ω, permanent elliptic shape (semiaxis a and b, $a>b$), and rotates around its center (say, $x=y=0$) with constant angular frequency $\Omega=\omega ab/(a+b)^2$. The individual fluid particles in this vortex move on *circular*, off-center trajectories with angular frequency 2Ω. In the present paper we shall describe a method of controlling the axis ratio $\rho\equiv a/b$ and rotation phase of the Kirchhoff vortex by placing it in a straining flow $u(x,t)\equiv\dot{x}=\varepsilon x$; $v(y,t)\equiv\dot{y}=-\varepsilon y$, where spatially uniform strain rate $\varepsilon(t)=\varepsilon_0+\varepsilon_1\cos\psi(t)$ is *small* (i.e., $\varepsilon/\omega\ll 1$), oscillates in time, and has a *slowly varying* frequency $\Lambda(t)\equiv\dot{\psi}$. Kida [2] showed that the presence of the strain still allows elliptic patch solutions, but the values of a and b and angle θ between the major axis a and the x axis are governed by

$$\dot{a}=\varepsilon a\cos(2\theta),\quad \dot{b}=-\varepsilon b\cos(2\theta),$$

$$\dot{\theta}=\Omega-\varepsilon[(a^2+b^2)/(a^2-b^2)]\sin(2\theta). \tag{1}$$

Steady-state solutions of this dynamical system with constant ε were studied by Moore and Saffman [3]; Kida [2] considered the unsteady case, and Neu [4] generalized the problem to include stretching along the rotation axis of the vortex in a three-dimensional strain. Here, we study evolution of Kirchhoff vortices in a straining flow with oscillating strain rate, as these oscillations resonate at $\Lambda=2\Omega$ with the particles in the vortex flow. We shall exploit nonlinear phase-locking (autoresonance) phenomenon in manipulating the vortex by chirping the frequency Λ of the strain rate. In the past, autoresonance was used in particle accelerators [5], atomic physics [6], nonlinear dynamics [7], and waves [8], so the present paper comprises an extension of autoresonance ideas to fluid dynamics. In particular, we shall show that, within the elliptic model, by using a *weak* straining flow ($\varepsilon/\omega\ll 1$) and starting from a circular ($\rho=1$) vortex, one can significantly increase the axis ratio ρ by slowly *lowering* the frequency of oscillations of the strain rate. In real applications, this result must pass stability test with respect to small deviations from the elliptic vortex model. The classical Love's work [9] shows that freely rotating Kirchhoff vortices become unstable with respect to boundary perturbations for $\rho>3$. A similar problem in the presence of a straining flow was studied by Dritschel [10], who showed that the effect of a weak strain on stability is small. Thus, the suggested autoresonant control of elliptic vortices is applicable to moderate axis ratios, $\rho<3$. The scope of our presentation will be as follows. In Sec. II we shall discuss various evolution stages of autoresonant elliptic vortices, and illustrate the theory by numerical examples. Section III will summarize our conclusions.

II. RESONANT VORTEX DYNAMICS

Since equations (1) conserve the area of the ellipse, the vorticity ω is conserved and we have only two independent variables in the problem. The convenient set of such variables is the axis ratio ρ and θ for which Eq. (1) yields

$$\dot{\rho}=2\varepsilon\rho\cos(2\theta),$$

$$2\dot{\theta}=2\Omega-2\varepsilon[(\rho^2+1)/(\rho^2-1)]\sin(2\theta), \tag{2}$$

where $\Omega\equiv\omega\rho(\rho+1)^{-2}$. We assume that all the parameters and time in Eq. (2) are normalized and set to be dimensionless. The natural normalization in our system is obtained by using some characteristic (fixed) value α of the rate of change of the driving frequency, so the dimensionless time in Eq. (2) is $\tau\equiv\alpha^{1/2}t$, while ω,ε (and later Λ) are $\alpha^{-1/2}\omega$, $\alpha^{-1/2}\varepsilon$ (and $\alpha^{-1/2}\Lambda$) in previous notations. Suppose that initially, at $\tau=\tau_0$, one starts with a circular [$\rho(\tau_0)=1$] vortex, while the oscillation frequency $\Lambda(\tau_0)$ of the strain rate is far from the resonant value $\Lambda_r=\omega/2=2\Omega_{p=1}$. Suppose also that $\Lambda(t)$ *decreases* in time and passes Λ_r at $\tau=\tau_r$ (we shall set $\tau_r=0$ in the following). A typical evolution, illustrating the autoresonance in our system in this case, is presented in Fig. 1. The figure shows the numerical solutions of Eq. (2) for ρ and the phase mismatch $\Phi=2\theta-\psi(\tau)$ (mod2π) in the case of linearly decreasing driving frequency, $\Lambda=\frac{1}{2}\omega-\tau$, i.e., $\psi=\psi_0+\frac{1}{2}\omega\tau-\frac{1}{2}\tau^2$. The parameters in these calculations were $\omega=100$, $\varepsilon_{0,1}=0.25$, $\psi_0=0$ and initial conditions $\rho=1+\sigma$, $\sigma\ll 1$, and $\theta=0$, at $\tau_0=-20$. We added σ in the initial condition because the phase equation in (2) has a singularity at $\rho=1$ and one must be careful in solving the sys-

*FAX: (972)-2-651-2483. Electronic address: lazar@vms.huji.ac.il

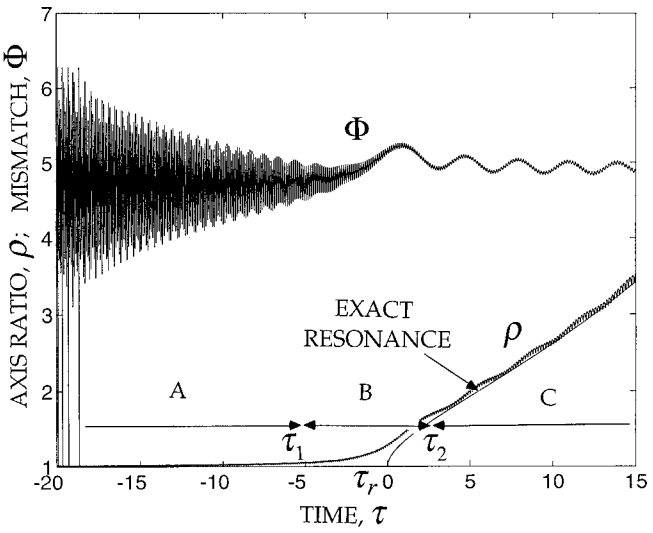

FIG. 1. The axis ratio $\rho=a/b$ and mismatch $\Phi=2\theta-\psi$ (mod2π) versus dimensionless time τ for linearly decreasing driving frequency, $\Lambda=\frac{1}{2}\omega-\tau$. The system evolves in three stages: the initial phase trapping stage (region *A*), weakly nonlinear stage (region *B*), and fully nonlinear autoresonance (region *C*). The smooth curve starting at $\tau=0$ is the exact resonance line $2\Omega(\rho)=\Lambda(\tau)$.

tem numerically. We used $10^{-6}<\sigma<10^{-4}$ with no visible differences from the results shown in Fig. 1. One can see in Fig. 1 that shortly beyond τ_0, the vortex rotation phase locks to that of the oscillations of the straining flow [at $\Phi\approx 3\pi/2$ (mod2π)], while for $\tau>0$ the axis ratio changes significantly, but preserves the approximate resonance condition $\Lambda(\tau)\approx 2\Omega[\rho(\tau)]$ continuously, despite the variation of Λ (the exact resonance curve, starting at $\tau=0$, is shown in the figure for comparison). We also see that the solutions have slowly evolving averages and superimposed small, rapidly varying oscillations. The analysis of the *slow* phase-locked evolution, which is the signature of the autoresonance in the system, comprises our main goal in the following. To simplify this analysis we shall formally split the evolution into three stages. In the first stage, at early times, $\tau_0\leqslant\tau\leqslant\tau_1<\tau_r$ (region *A* in the figure), when the system is still far from the resonance, $\rho\approx 1$ and we can neglect the variation of Ω with time, i.e. set $\Omega\approx\omega/4$ in the equation for $\dot{\theta}$ in Eq. (2). This simplified system predicts (see below) strong phase locking between the rotation phase of the vortex and that of the driving oscillations as one approaches $\tau\approx\tau_1$. We shall use the term *initial phase trapping stage* to describe this early evolution. Beyond τ_1 one must include the ρ dependence in Ω. However, since in region *B* in the figure ($\tau_1<\tau<\tau_2$), ρ is still close to unity, one can use small $\delta\equiv\rho-1$ expansion of Ω to $O(\delta^2)$. This is the *weakly nonlinear* autoresonant evolution stage. We shall show that the small parameter ε/ω must be above a certain *threshold* for having persisting autoresonance in the weakly nonlinear evolution stage. Finally, beyond τ_2 (region *C*), as the autoresonance (phase locking) continues, the elongation of the ellipse becomes significant and one must use the full ρ dependence in Ω. We shall see that there exists a uniform approach for studying autoresonance in both regions *B* and *C*. Nevertheless, in region *C*, the problem can be simplified by neglecting the interaction term in the equation for $\dot{\theta}$. We shall use the term *fully nonlinear* autoresonance to describe the system's evolution in this case. The detailed analysis of these different stages of vortex dynamics is presented below.

A. Initial phase trapping stage

We use small $\delta\equiv\rho-1$ expansion in Eq. (2) to describe weak deformations of the vortex from initially circular profile, as one passes through resonance with the oscillating strain rate. Then, to $O(\delta^2)$,

$$\dot{\delta}=2\varepsilon\cos(2\theta),$$

$$2\dot{\theta}=\tfrac{1}{2}\omega\left(1-\tfrac{1}{4}\delta^2\right)-2\varepsilon\delta^{-1}\sin(2\theta). \tag{3}$$

We shall neglect the δ^2 term in Eq. (3) in the initial phase trapping stage (but include it later in studying the weakly nonlinear interaction). Then, Eq. (3) can be rewritten as a single equation for $Z\equiv\delta\exp(2i\theta)$:

$$\dot{Z}=i(\omega/2)Z+2\varepsilon. \tag{4}$$

The solution of this equation (with zero initial conditions) is $Z=2\int_{\tau_0}^{\tau}\varepsilon(\tau')\exp[i\omega(\tau-\tau')/2)]d\tau'$. For further progress one must specify the time dependence in $\varepsilon(\tau)=\varepsilon_0+\varepsilon_1\cos\psi(\tau)$. For simplicity, as in Fig. 1, we shall assume the linear dependence of the driving frequency $\Lambda(\tau)=\omega/2-\tau$, so $\psi=\psi_0+\frac{1}{2}\omega\tau-\frac{1}{2}\tau^2$. Then, upon integration,

$$Z=4i(\varepsilon_0/\omega)[1-e^{i(\omega/2)(\tau-\tau_0)}]+i\varepsilon_1\sqrt{\pi}e^{1/2i\omega\tau}\{e^{i\psi_0}[F(\tau)]_{\tau_0}^{\tau}+e^{-i(\omega_0+\omega^2/2)}[F^*(\tau)]_{\tau_0-\omega}^{\tau-\omega}\},$$

where $F(\tau)\equiv[f(\tau/\sqrt{\pi})+ig(\tau/\sqrt{\pi})]\exp(-i\tau^2/2)$, and f and g are the auxiliary functions associated with Fresnel integrals $C(z)$ and $S(z)$ [11]. For $|\tau|\gg 1$, f and g scale as $f\sim\pi^{-1/2}\tau^{-1}$ and $g\sim\pi^{-1/2}\tau^{-3}$, so, if $|\tau_1|\gg 1$, we can write $F(\tau)\approx\pi^{-1/2}\tau^{-1}\exp(-i\tau^2/2)$ in the initial excitation stage. Then, if $\tau_{0,1}\ll\omega$ (conditions assumed to be satisfied in the following), we get an approximation $Z=4i(\varepsilon_0/\omega)[1-e^{i(\omega/2)(\tau-\tau_0)}]+i\varepsilon_1 e^{i\psi(\tau)}[\tau^{-1}-\tau_0^{-1}e^{i1/2(\tau^2-\tau_0^2)}]$ for $\tau_0<\tau<\tau_1$. Finally, by defining the phase mismatch $\Phi\equiv 2\theta-\psi(\tau)$ between twice the rotation angle of the elliptic vortex and the phase of the driving oscillation, we obtain

$$\delta\exp[i(\Phi-\pi/2)]=-iZ\exp[-i\psi(\tau)]=\varepsilon_1/\tau+D, \tag{5}$$

where

$$D=(4\varepsilon_0/\omega)e^{-i\psi}[1-e^{i(\omega/2)(\tau-\tau_0)}]-\varepsilon_1\tau_0^{-1}e^{i1/2(\tau^2-\tau_0^2)}.$$

Note that both $\mathrm{Re}\,D$ and $\mathrm{Im}\,D$ oscillate around zero, but remain bounded, since $|\mathrm{Re}\,D,\mathrm{Im}\,D|<(8\varepsilon_0/\omega)+(\varepsilon_1/|\tau_0|)$. On the other hand, $\varepsilon_1/|\tau|$ in Eq. (5) grows as τ moves towards τ_1. The phase trapping occurs when $\varepsilon_1/|\tau|$ becomes larger than the upper bound on $|\mathrm{Re}\,D|$ and not later than $\tau=\overline{\tau}\equiv-\varepsilon_1[(8\varepsilon_0/\omega)+(\varepsilon_1/|\tau_0|)]^{-1}$. Our example ($\varepsilon_{0,1}=0.25$, $\omega=100$, $\tau_0=-20$) yields the trapping prior $\overline{\tau}\approx-7.7$. Beyond the trapping point as $|\tau|$ continues to decrease and approaches $|\tau_1|$, the first term in Eq. (5) becomes dominant and one obtains an approximation $\delta\exp[i(\Phi-\pi/2)]\approx\varepsilon_1/\tau$. Thus, for negative τ, $\delta\to\varepsilon_1/|\tau|$ and $\Phi\to 3\pi/2$ (mod2π), as τ approaches τ_1. In other words, twice the rotation angle of the

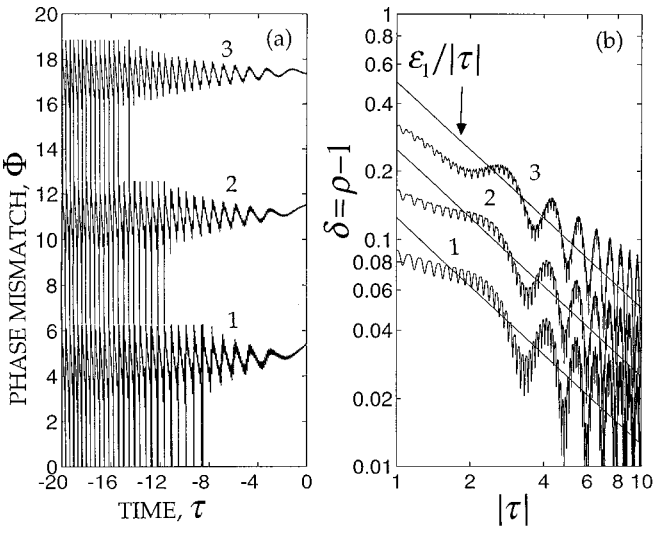

FIG. 2. The evolution of the phase mismatch Φ (mod2π) [Fig. 2(a)] and $\delta=\rho-1$ [Fig. 2(b)] in the initial phase trapping stage. The curves 1, 2, and 3 correspond to three different strain rate oscillation amplitudes $\varepsilon_1=0.125$, 0.25, and 0.5, respectively. The phase mismatch curves for $\varepsilon_1=0.25$ and 0.5 are shifted by 2π and 4π, respectively, for better disposition. The straight lines in Fig. 2(b) are curves $\varepsilon_1/|\tau|$.

elliptic vortex locks to the phase of oscillations of the driving strain rate, i.e., the fluid particles *resonate* with the driving oscillation. We illustrate our predictions in Fig. 2, showing the numerical results for Φ [Fig. 2(a)] and δ [Fig. 2(b)] versus time for the same parameters as in Fig. 1, but for $\varepsilon_0=0.125$, $\psi_0=\pi$ and three values of $\varepsilon_1=0.125$, 0.25, 0.5 (curves 1, 2, and 3, respectively). One can see in the figure that in all the cases, the phase trapping starts not later than $\overline{\tau}$ defined above and, at some $\tau_1<0$, $\Phi\to 3\pi/2$ (mod2π) while $\delta\to\varepsilon_1/|\tau|$ [the straight lines in Fig. 2(b)]. One can also see in the figure that τ_1 can be chosen so that δ is still small (say, $\delta<0.1$) justifying the linear analysis. For instance, in Fig. 2, $\tau_1=-3$, -5, -8 for the cases 1, 2, and 3, respectively. Since beyond τ_1, δ continues to increase, we shall include the nonlinearity in the problem for $\tau>\tau_1$. Nevertheless, we can use the relative smallness of δ for some time and start the analysis within a weakly nonlinear formalism. Note that the linear analysis is still valid at τ_1 and, therefore, the transition to the weakly nonlinear theory at τ_1 is continuous with no need in studying an intermediate case.

B. Weakly nonlinear evolution

Beyond the initial *linear* phase locking stage described above, we include the δ^2 term in the second equation in (3) to properly describe the weak nonlinear dynamics at $\tau>\tau_1$. Assuming the continuing phase locking in the system we use Eq. (3) to write *slow* equations for δ and $\varphi\equiv\Phi-3\pi/2$,

$$\dot{\delta}=\varepsilon_1\sin\varphi,$$

$$\dot{\varphi}=\tau-\tfrac{1}{8}\omega\delta^2+\varepsilon_1\delta^{-1}\cos\varphi. \tag{6}$$

Here we have discarded the rapidly varying *nonresonant* interaction terms (these are the terms responsible for the fast oscillations in Fig. 1 around the slow solutions), i.e., replaced $\varepsilon\cos(2\theta)$ and $\varepsilon\sin(2\theta)$ by $\frac{1}{2}\varepsilon_1\cos\Phi$ and $\frac{1}{2}\varepsilon_1\sin\Phi$, respectively. Now, we seek solution of Eq. (6), where $\varphi(\tau)$ is continuously small ($|\varphi|\ll 1$) and, to lowest order, set $\cos\varphi\approx 1$ in the second equation in (6), i.e., use

$$\dot{\varphi}\approx\tau-\tfrac{1}{8}\omega\delta^2+\varepsilon_1/\delta. \tag{7}$$

Furthermore, we shall write $\delta=d(\tau)-\Delta(\tau)$, where the monotonically varying part $d(\tau)$ is defined by equating the right-hand side of Eq. (7) to zero, i.e., $\tau-\frac{1}{8}\omega d^2+\varepsilon_1/d\equiv 0$, while $\Delta(\tau)$ is assumed to be small ($|\Delta|/d\ll 1$). Then, by linearization,

$$\dot{\Delta}=S^{-1}-\varepsilon_1\sin\varphi,\quad \dot{\varphi}=S\Delta, \tag{8}$$

where $S(t)\equiv\frac{1}{4}\omega d+\varepsilon_1/d^2$. The Hamiltonian for this dynamical system is $H\equiv\frac{1}{2}S\Delta^2+V_{eff}(\varphi)$, with the effective potential $V_{eff}\equiv-\varphi/S-\varepsilon_1\cos\varphi$. The slow time dependence enters H parametrically via d. The necessary condition for having *stable* solutions of Eq. (8) is the existence of trapped phase space regions for values of d in the region of interest. Thus we require $\varepsilon_1 S>1$ in the weakly nonlinear evolution stage. On the other hand, S has a minimum $S_m=\frac{3}{4}(\varepsilon_1\omega^2)^{1/3}$ at $d=d_m=2(\varepsilon_1/\omega)^{1/3}$. Therefore, the necessary condition for stability is $\varepsilon_1 S_m>1$, yielding the threshold condition on the strain rate:

$$\varepsilon_1>\varepsilon_{th}=(\tfrac{4}{3})^{3/4}\omega^{-1/2}. \tag{9}$$

[Note that if one returns to the dimensional parameters by replacing $\omega\to\alpha^{-1/2}\omega$ and $\varepsilon_1\to\alpha^{-1/2}\varepsilon_1$, condition (9) becomes $\varepsilon_1>(\frac{4}{3}\alpha)^{3/4}\omega^{-1/2}$, where ε_1, ω, and $\alpha^{1/2}$ have the usual dimension of $\sec^{-1}$.] In addition to Eq. (9), one must impose the adiabaticity condition $|\dot{\nu}|\nu^{-2}<1$ on the rate of variation of the characteristic frequency $\nu\approx(\varepsilon_1 S)^{1/2}$ of the oscillations of φ and Δ. These two conditions are sufficient for having the autoresonance (i.e., continuing and stable phase locking $\varphi\approx 0$) in our system. Simple analysis shows that $|\dot{\nu}|\nu^{-2}=\varepsilon_1^{-1/2}S^{-5/2}d^{-1}(\frac{3}{8}\omega d-S)$ reaching, at $d\approx d_m/2$ the absolute maximum value $\sim\frac{1}{2}(\varepsilon_1^2\omega)^{-2/3}$, so the adiabaticity condition yields $\varepsilon_1>(0.5)^{3/4}\omega^{-1/2}$, which has the same scaling as Eq. (9), but is slightly less restrictive. Thus condition (9) is both necessary and sufficient for autoresonance in the weakly nonlinear interaction stage. Numerical calculations indicate that this threshold is rather sharp. Figure 3 shows the results of numerical solutions of Eq. (2) in two cases, where all the parameters are as those in Fig. 1, but $\varepsilon_1=0.114$ (curves 1) and $\varepsilon_1=0.134$ (curves 2), i.e., below and above the threshold value $\varepsilon_{th}=0.124$ for our case. One can see that the phase locking discontinues at $\tau\approx 2$ for $\varepsilon_1<\varepsilon_{th}$, preventing fully nonlinear autoresonance in the system, while the growth of ρ saturates shortly after the dephasing. A different characteristic signature of the transition to autoresonance is illustrated in Fig. 4, showing the dependence of the axis ratio ρ at the final integration time ($\tau=15$) on the amplitude of the oscillations ε_1 of the strain rate. We used two values of vorticity in these calculations [$\omega=100$ (circles) and $\omega=200$ (triangles)], while all other parameters and initial conditions (at $\tau=-20$) are the same as in Fig. 1. We see that below the threshold (indicated by

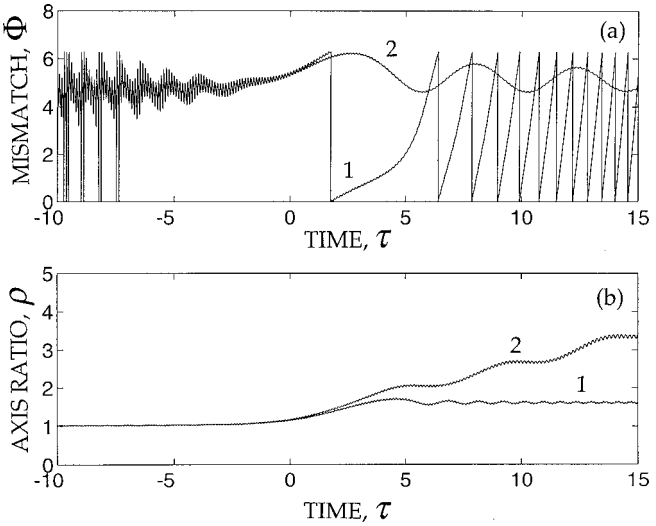

FIG. 3. The evolution of the system below (curves 1, $\varepsilon_1 = 0.114$) and above (curves 2, $\varepsilon_1 = 0.134$) the threshold value ($\varepsilon_{th} = 0.124$) given by Eq. (9). (a) Phase mismatch versus time. (b) Axis ratio versus time. The dephasing takes place when $\varepsilon_1 < \varepsilon_{th}$ and the autoresonance discontinues.

vertical lines in the figure), the final value of ρ is almost independent of ω, as should be in the linear theory. In the vicinity of the predicted threshold, the final amplitude jumps to the value, approximately satisfying the nonlinear resonance condition $2\Omega(\rho) = \Lambda(\tau)$ at the final integration time. The transition to fully nonlinear autoresonant evolution takes place at intermediate times and we proceed to the analysis of this stage.

C. Fully nonlinear autoresonance

The weakly nonlinear theory allowed a simple description of the autoresonance threshold problem yielding expression (9). However, one can use similar ideas in developing a *uniform* description of both the weakly and strongly nonlinear autoresonance. We need only the initial phase locking assumption in this development (recall that the phase locking is established during the initial linear interaction stage). Indeed, let us return to the original system (2); assume (starting $\tau = \tau_1$) the continuing phase locking in the system and write the *slow* equations for ρ and $\varphi = \Phi - 3\pi/2$ [compare to Eqs. (6) and (7)]:

$$\dot{\rho} = \varepsilon_1 \rho \sin\varphi, \quad \dot{\varphi} = \tau - F(\rho), \tag{10}$$

where $F = \omega/2 - 2\Omega(\rho) - \varepsilon_1(\rho^2+1)/(\rho^2-1)$. Next, we write $\rho = \rho_0(\tau) - \Delta(\tau)$, where $\rho_0(\tau)$ is defined via $F[\rho_0(\tau)] \equiv \tau$ and assume that $|\Delta(t)|/\rho_0 \ll 1$. Then, by linearization, Eqs. (10) yield [compare to the weakly nonlinear system (8)]

$$\dot{\Delta} = G^{-1} - \varepsilon_1 \rho_0 \sin\varphi, \quad \dot{\varphi} = G\Delta, \tag{11}$$

where $G \equiv dF/d\rho_0 = 2\omega(\rho_0-1)(\rho_0+1)^{-3} + 4\varepsilon_1\rho_0(\rho_0^2-1)^{-2}$. Equations (11) again comprise a Hamiltonian system with $H = \frac{1}{2}G\Delta^2 + V_{eff}$ and $V_{eff} = -\varphi/G - \varepsilon_1\rho_0\cos\varphi$. For small values of $\delta = \rho_0 - 1$, the problem reduces to that studied in the weakly nonlinear stage, because $G \to S$ in this limit. Now, we observe that G is positive, so $F(\rho_0)$ is an *increasing* function of ρ_0 and, therefore, ρ_0 is an *increasing* function of time. The necessary condition for having stable oscillations of Δ and φ is $\varepsilon_1\rho_0 G > 1$. As in the weakly nonlinear theory, this condition guarantees the existence of a trapped region in the (Δ,φ) phase space. One finds that function $\rho_0 G$ has a minimum at small δ and a maximum at $\rho_0 \approx 3.7$. We are interested in the range $1 \leqslant \rho_0 < 3$ to avoid the instability of the elliptic vortex boundary [9]. In this range, the condition $\varepsilon_1\rho_0 G > 1$ is most difficult to satisfy at the minimum of $\rho_0 G$ at small values of δ. This yields the threshold condition (9) as discussed previously. Above the threshold, when ρ_0 increases with time, the system remains in the trapped state (oscillating Δ and φ), provided the variation of ρ_0 is sufficiently slow. In other words, for having continuing autoresonance, one must also satisfy the adiabaticity condition

$$|\dot{\nu}|\nu^{-2} < 1, \tag{12}$$

where $\nu^2 = \varepsilon_1\rho_0 G$ is the characteristic frequency of small autoresonant oscillations. We have already analyzed this condition in the weakly nonlinear limit and showed that the left-hand side of Eq. (12) reaches the maximum of $\frac{1}{2}(\varepsilon_1^2\omega)^{-2/3}$ at $\rho_0 \approx 1 + (\varepsilon_1/\omega)^{1/3}$. When ρ_0 increases beyond this maximum, the adiabaticity condition is first easier to satisfy. Later, the analysis can be simplified for ρ_0 large enough to neglect the interaction term in the expression for $F(\rho_0)$. Then, the relation $F(\rho_0) \approx \omega/2 - 2\Omega(\rho_0) = \tau$ is equivalent to the exact resonance condition $\Omega_0 \equiv \Omega(\rho_0) = \frac{1}{2}\Lambda(\tau)$. This equivalence explains the satisfaction of the *approximate* resonance condition $\Omega(\rho) = \frac{1}{2}\Lambda(\tau)$ by the system in the advanced autoresonance stage (beyond $\tau = 0$), as illustrated in the example in Fig. 1. Within the same approximation of $F(\rho_0)$, we find $\nu^2 \approx -2\varepsilon_1\rho_0\Omega_0' = 2\varepsilon_1\omega\rho_0(\rho_0-1)(\rho_0+1)^{-3}$. Then $|\dot{\nu}|\nu^{-2} = 0.177(\varepsilon_1\omega^3)^{-1/2}\rho_0^{-3/2}|\rho_0^2 - 4\rho_0 + 1|(\rho_0+1)^{7/2}(\rho_0-1)^{-5/2}$. This function decreases

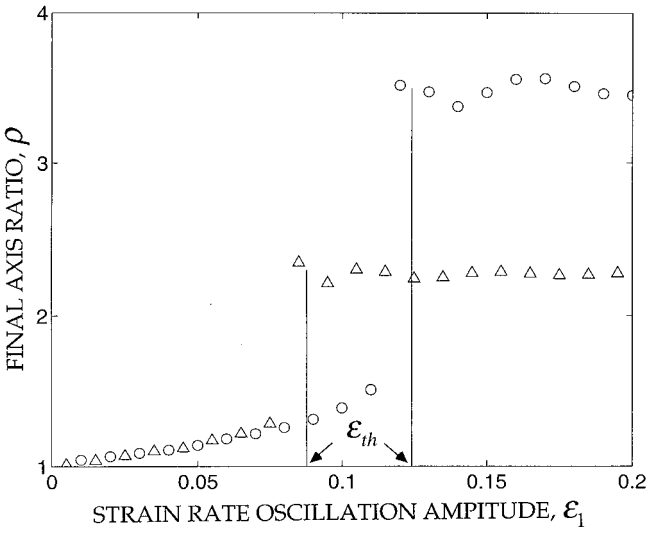

FIG. 4. The value of the axis ratio ρ at the final integration time $\tau = 15$ versus strain rate oscillation amplitude ε_1 for two vorticity cases $\omega = 100$ (circles) and $\omega = 200$ (triangles). Other parameters are the same as in Fig. 1. The vertical lines show the position of the theoretical threshold ε_{th} [see Eq. (9)] for autoresonance.

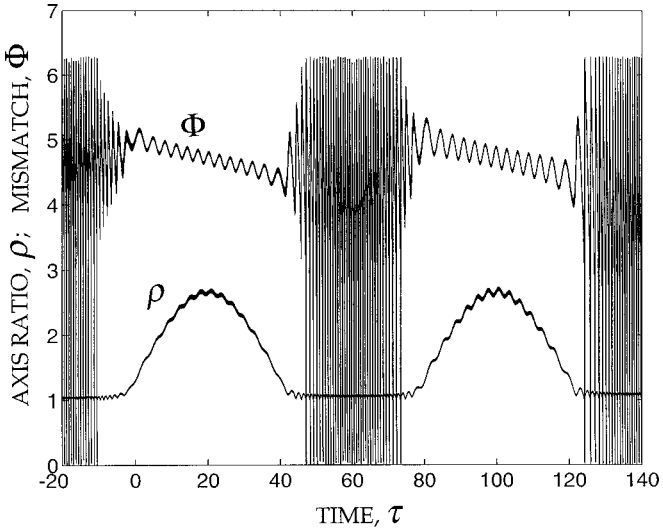

FIG. 5. The evolution of the system for oscillating chirp, $\Lambda = \frac{1}{2}\omega + \Lambda_0 \sin(\pi\tau/2T)$, of the frequency of the strain rate. Repetitive autoresonant excitations during two successive periods of oscillations of Λ are shown.

with ρ_0 in the range of interest ($1<\rho_0<3$). Therefore, the adiabaticity condition (12) is easier to satisfy in the fully nonlinear regime with the increase of ρ_0 in this range. Note that within our Hamiltonian picture, the product $I = (\Delta)_{\rm amp}(\varphi)_{\rm amp}$ of the amplitudes of oscillations of the dependent variables in Eq. (11) is an adiabatic invariant. In the fully nonlinear regime, one finds [see the second equation in (11)] that $(\varphi)_{\rm amp} \sim (2|\Omega_0'|I/\nu)^{1/2}$, while $(\Delta)_{\rm amp} = I/(\varphi)_{\rm amp} \sim (\frac{1}{2} I\nu/|\Omega_0'|)^{1/2}$. Therefore, the initial smallness of I guarantees the continuing smallness of the autoresonant oscillations.

We conclude our discussion of autoresonant elliptic vortices by demonstrating that the time dependence of the oscillation frequency $\Lambda(\tau)$ of the strain rate in autoresonance needs not be necessarily linear, as long as it is slow enough. This is illustrated in Fig. 5, presenting numerical solutions of Eq. (2) in the case when $\Lambda(\tau)$ oscillates around the linear resonance, i.e., $\Lambda = \frac{1}{2}\omega - \Lambda_0 \sin(\frac{1}{2}\pi\tau/T)$, with $\Lambda_0 = 10$ and $T = 20$, while other parameters and initial conditions are the same as in Fig. 1. The figure shows successive increases and decreases of the ellipticity of the vortex patch in two oscillation periods of $\Lambda(\tau)$. The figure also illustrates that, in the vicinity of the linear resonance, autoresonant excitations are unidirectional and the phase trapping occurs only when the driving frequency *decreases* as it passes the linear resonance frequency $\frac{1}{2}\omega$. In contrast, when the frequency increases at the linear resonance the dephasing takes place and, as expected, no autoresonance exists for Λ larger than $\frac{1}{2}\omega$.

III. CONCLUSIONS

We have studied autoresonant evolution of Kirchhoff vortices driven by a weak strain with oscillating strain rate and chirped oscillation frequency $\Lambda(t)$. In autoresonance, the system self-adjusts the axis ratio of the vortex, so that twice the rotation phase of the ellipse is continuously locked to that of the oscillating strain rate despite the variation of Λ. The initial phase locking in the system is an important ingredient in having the autoresonance and requires starting with nearly circular vortex and passing the linear resonance $\Lambda = \omega/2$ by slowly decreasing $\Lambda(t)$. The oscillation amplitude of the strain rate must be sufficiently small, but also satisfy the threshold condition (9). In dimensional notations, these requirements can be written as $1 \gg \varepsilon_1/\omega > (4\alpha/3\omega^2)^{3/4}$ and guarantee both the perturbative character of autoresonant interaction and stability during the weakly nonlinear evolution stage. Furthermore, the adiabaticity condition (12) must be satisfied for sustaining autoresonance in the strongly nonlinear stage, where the elongation of the elliptic vortex becomes significant. Finally, at axis ratio $\rho_0 > 3$, similarly to free Kirchhoff vortices [9], we expect the autoresonant solution to become unstable with respect to perturbations of the elliptic vortex boundary.

Our theory can be generalized to include the possibility of time varying vorticity $\omega(t)$, when one adds the axial straining flow velocity component, i.e., uses the strain $\dot{x} = \varepsilon_x x$, $\dot{y} = -\varepsilon_y y$, $\dot{z} = \varepsilon_z z$ [4], where $\varepsilon_x - \varepsilon_y + \varepsilon_z = 0$ for continuity. Also, instead of oscillating the strain rate, one can use $\varepsilon = {\rm const}$, but add *slowly varying* uniform vorticity $2\gamma(t)$ in the perturbing flow $\dot{x} = \varepsilon x - \gamma y$, $\dot{y} = -\varepsilon y + \gamma x$. The evolution equations in this case are the same as Eq. (1) if Ω is replaced by $\Omega + \gamma(t)$ [2]. Therefore, we expect transition to autoresonance as $|\gamma|$ decreases and passes the linear resonance $2\gamma + \omega/2 = 0$ at some time. At later times, the axis ratio will continue to increase, in order to sustain the approximate nonlinear resonance relation $\Omega[\rho(t)] + \gamma(t) \approx 0$ with the decrease of $|\gamma|$. The vortex angle, in this case, remains nearly constant ($\theta \approx \pi/4$), as the axis ratio continues to grow. In addition to these applications, it seems interesting to implement autoresonant ideas in more complex vortex systems, such as vortices near walls or driven multiple vortex structures. Other challenging goals are inclusion of viscosity in the theory and experimental observation of autoresonant elliptic vortices.

ACKNOWLEDGMENT

This work was supported by the Israel Science Foundation founded by the Israel Academy of Sciences and Humanities.

[1] H. Lamb, Hydrodynamics, 6th ed. (Cambridge University Press, Cambridge, 1932), Sec. 159.
[2] S. Kida, J. Phys. Soc. Jpn. **50**, 3517 (1981).
[3] D. W. Moore and P. G. Saffman, in *Aircraft Wake Turbulence*, edited by J. Olson, A. Goldberg, and N. Rogers (Plenum, New York, 1971), pp. 339–354.
[4] J. C. Neu, Phys. Fluids **27**, 2397 (1984).
[5] M. Livingston, *High-Energy Accelerators* (Interscience, New York, 1954).
[6] B. Meerson and L. Friedland, Phys. Rev. A **41**, 5233 (1990).

[7] E.g., G. Cohen and B. Meerson, Phys. Rev. E **2**, 967 (1993).
[8] E.g., L. Friedland, Phys. Plasmas **5**, 645 (1998).
[9] A. E. H. Love, Proc. London Math. Soc. **25**, 18 (1893).
[10] D. G. Dritschel, J. Fluid Mech. **210**, 223 (1990).
[11] *Handbook of Mathematical Functions*, Natl. Bur. Stand. Appl. Math. Ser. No. 55, edited by M. Abramowitz and I. A. Stegun (U.S. GPO, Washington, D.C., 1968), p. 300.